Supplement of Biogeosciences, 14, 2283–2292, 2017
http://www.biogeosciences.net/14/2283/2017/
doi:10.5194/bg-14-2283-2017-supplement
© Author(s) 2017. CC Attribution 3.0 License.

Biogeosciences
Open Access

Supplement of

The origin of methane in the East Siberian Arctic Shelf unraveled with triple isotope analysis

Célia J. Sapart et al.

Correspondence to: Célia J. Sapart (csapart@ulb.ac.be)

The copyright of individual parts of the supplement might differ from the CC-BY 3.0 licence.

SUPPLEMENTARY INFORMATION

1. DEEP CORE LITHOLOGY

Table S1 shows the coordinates, bathymetry, distance from the coast and inundation time data of the deep cores. The major differences in the lithology of the deep cores drilled in 2011 and 2013 are the thickness and the origin of the Holocene age sediment. In the non-ebullition core, Holocene age marine sediments compose the upper 5.5m. They represent disperse pelite-aleurite deposits predominantly of alluvial origin, which are accumulations of river-derived matter formed in coastal marine conditions with high rates of sediment accumulation (Fig.S1). Holocene sediments are underlain with terrestrial accumulations (5.8m to 52.3m) of late Pleistocene age, which are represented by consolidated aleuro-sands inter-layered by fine-grained aleurite accumulations with inclusions of pebbles and wood remains.

The other deep cores (the hotspot cores) were drilled in 2013 near the Muostakh Island. In the IID-13 and IIID-13 cores, the Holocene age sediments represent only the upper 0.5m and consist of remains of the coastal ice-complex (IC or Yedoma) of Muostakh Island. This area represents a former part of the coastal alluvial plain, the upper part of which is composed of IC that thaws very fast during the last century. Sediment morphology reflects the nature of the sediments: fine-grained sand-aleurite-pelite is interlayered with gravel-pebble material with inclusions of wood remains and plant debris.

Sediment core VD-13 stands out of all the other cores drilled in 2013. Its morphological structure is different as its frozen fraction is presented by sands interlayered by gravel-pebble accumulations.

2. INTERPRETATION OF THE ^{14}C-CH_4 RESULTS

The observation of unexpectedly high ^{14}C values for the ID-11 non-ebullition core and water samples from the shelf edge needs further discussion. As explained in the main text, ^{14}C values >200pmC do not exist in nature in any carbonaceous material including CH_4, not even at the height of surface nuclear bomb tests of the mid-20th century. We assume that a local anthropogenic nuclear contribution is the most likely explanation for our elevated radiocarbon levels, which is justified in this section.

In the ID-11 non-ebullition sediment, the higher ^{14}C values correspond to the lower CH_4 concentrations (Fig. S5). That implies a possible mixture between a older CH_4 source and a background highly enriched in ^{14}C. A Keeling plot shows that the highly enriched ^{14}C contribution is relatively small in terms of CH_4 quantity and that the main CH_4 substrate is relatively old (Fig. S5). For the hotspot sites, where CH_4 concentrations are larger, no mixture with a “younger” source is identified. All data points are showing very low ^{14}C (<1.5pmC) so the main CH_4 substrate at these sites is clearly of Pleistocene age. Note that all points of the IID-13 core were below the analytical detection limit of 0.8pmC hence no conclusions could be drawn from the Keeling plot of this core.

The very high ^{14}C values >200pmC may either originate from *in situ* cosmogenic or nuclear production of radioactive CH_4 or its substrate. Enhanced ^{14}C has been found in meteorites (Firemann, 1978) and can be produced at the surface of ice sheets (e.g. Fireman and Norris et al., 1982), but in both cases, the quantity of ^{14}C formed is very small compare to what we observed in the Buor-Khaya Bay and shelf edge sediment and water samples. Nuclear production of ^{14}C involves formation by neutron activation as consequence of a nuclear chain reaction, which may either take place naturally or artificially. In the atmosphere, cosmic rays can also produce neutrons which can react with ^{14}N to produce ^{14}C. The only place on Earth, where evidence of a natural nuclear reactor has been found is in Oklo, Gabon (Baudin et al., 1972, Cowan, 1976, Kuroda, 1982). However, such natural reactors cannot be active anymore today, as the relative abundance of fissile ^{235}U has now decayed below that required threshold for a sustainable nuclear reaction chain.

The Arctic Ocean has been used as a disposal area for radioactive wastes (Nuclear Wastes in the Arctic report, 1995, Johnson-Pyrtle and Scott, 1991). We therefore believe that anthropogenic nuclear contamination is the most likely explanation for these ^{14}C-enriched CH_4 background contribution. Similar cases but with slightly lower values have been observed in gas samples from marine basins along the Californian coast (Kessler et al., 2008). We suggest that nuclear anthropogenic contamination could have been laterally transported from thawing terrestrial permafrost in the pore-water of the thawing subsea permafrost in the form of CH_4 or of one of its precursors (e.g. dissolved inorganic carbon) to our drilling site and further on the shelf. Note that more data, e.g. of other radionuclides would be essential to confirm this interpretation.

We exclude a possible contamination during sampling, extraction and analysis, because no radioactive tracers were used during the sampling expeditions. The samples affected by enriched ^{14}C values were not sampled in a similar manner. The sediment samples were drilled from the ice in 2011 while the shelf edge water samples were sampled in 2012 from a ship together with other water and surface sediment samples showing no enrichment in ^{14}C values. For the rest of the sampling and analysis process, all samples were handled in a similar way and measured in a random order, but only samples from these two specific locations show highly enriched ^{14}C values. None of the reference and blank measurements were abnormal either.

SUPLEMENTARY REFERENCES

Baudin, G., Blain, C., Hagemann, R., Kremer, M., Lucas, M., Merlivat, L., Molina, R., Nieff, G., Prost Marechal, P., Regnaud, F. & Roth, E.: Quelques données nouvelles sur les reactions nucléaires en chaine que se sont produites dans le gisement d'Oklo, C.R. Acad. Sci. Paris, 275D, 2291, 1973.

Cowan, George A.: A natural fission reactor, Scientific American, 235.1, 36-47,1976.

Firemann, E. L.: Carbon-14 in lunar soil and in meteorites, Proc. Lunar Planet. Sci. Conf. 9th, 1647-1654, 1978.

Fireman, E.L., and Norris, T.L.: Ages and composition of gas trapped in Allan Hills and Byrd core, Earth and Planetary Science Letters, 60, 339-350, 1982.

Johnson-Pyrtle, A. and Scott, M.R.: Distribution of 137 Cs in the Lena River Estuary-Laptev Sea System, Marine Pollution Bulletin Vol. 42, No. 10, pp. 912-926, 2001.

Kessler, J. D., Reeburgh, W.S., Valentine, D.L., Kinnaman, F.S., Peltzer, E.T., Brewer, P.G., Southon, J. & Tyler, S.C.: A survey of methane isotope abundance (^{14}C, ^{13}C, ^{2}H) from five nearshore marine basins that reveals unusual radiocarbon levels in subsurface waters, J. Geophys. Res.,113, C12021, 2008.

Kuroda, P. K.: The Oklo phenomenon." The Origin of the Chemical Elements and the Oklo Phenomenon, Springer Berlin Heidelberg, 31-55, 1982.

Nuclear Wastes in the Arctic: An Analysis of Arctic and Other Regional Impacts from Soviet Nuclear Contamination, OTA-ENV-623 (Washington, DC: U.S. Government Printing Office, September), 1995.

SUPLEMENTARY FIGURES AND TABLE

Borehole/shelf area of sampling	Latitude	Longitude	Water depth, m	Water temperature surface/ bottom	Water salinity surface/ bottom	Time since inundation	Distance from the shore, km
ID-11	71,6926	130,3669	12.5	-0.52/-0.92	10.8/19.4	~8÷7 kyr BP	18.6 km from Muo-stakh Isl and 39.8 km from Bykovsky Peninsula
IID-13	71,6288	129,8534	2.5	-0.41/-0.61	12.8/13.2	~7÷6 kyr BP	2.5 km
IIID-13	71,6219	129,8517	4.1	-0.40/-0.61	12.8/13.2	~7÷6 kyr BP	2.5 km
VD-13	71,7449	129,4048	3.6	-1.01/-1.03	22.6/22.6	Lagoon, ~7÷6 kyr BP (Romanovsky et al., 1999)	Lagoon adjacent to the coast
Lena Delta						~7÷6 kyr BP	-
Str. 42*	72,977	130,141	12.5	3.74/1.42	16.3/22.3		
47*	72,427	130,151	8.5	4.42/2.53	0.5/4.6		
70**	72.687	130.640	20	2.40/2.83	19.0/21.5		
71**	72.683	130.267	12	1.02/2.47	9.0/19.1		
Dmitry Laptev						~8÷7 kyr BP	-
Str. 31*	72,882	140,620	15.5	3.38/3.76	18.7/20.3		
36*	73,118	139,517	13.5	3.30/3.44	19.8/24.0		
79**	73.030	139.393	15.0	1.92/3.04	19.8/23.3		
80**	73.169	139.574	15	1.67/2.42	19.3/26.7		
81**	73.316	139.768	9	1.85/1.79	18.6/24.8		
82**	73.297	140.085	11	1.6/1.46	24.17/26.4		
83**	73.104	140.352	14	1.75/2.19	20.3/26.5		
84**	72.930	140.619	12	1.77/1.77	21.1/21.1		
85**	72.886	140.643	24	1.69/1.77	20.8/20.9		
Buor-Khaya Gulf	Drilling sites					~8÷7 kyr BP	-
Shelf edge						~15÷13 kyr BP	-
Sts. 9*	76,897	127,8047	62	3.54/-1.33	28.0/33.4		
13*	76,894	127,8032	63	3.47/-1.40	29/1/33.3		
28**	77.000	125.985	91	3.87/-0.82	28.8/34.4		
32**	77.029	127.289	74	3.00/-1.21	21.9/34.2		
36**	76.398	125.051	62	1.26/-1.17	19.0/34.1		
37**	76.648	125.048	70	1.89/-1.19	17.3/34.2		

Table S1: Coordinates, bathymetry, temperature, salinity, distance from the coast and inundation time for all sample locations.

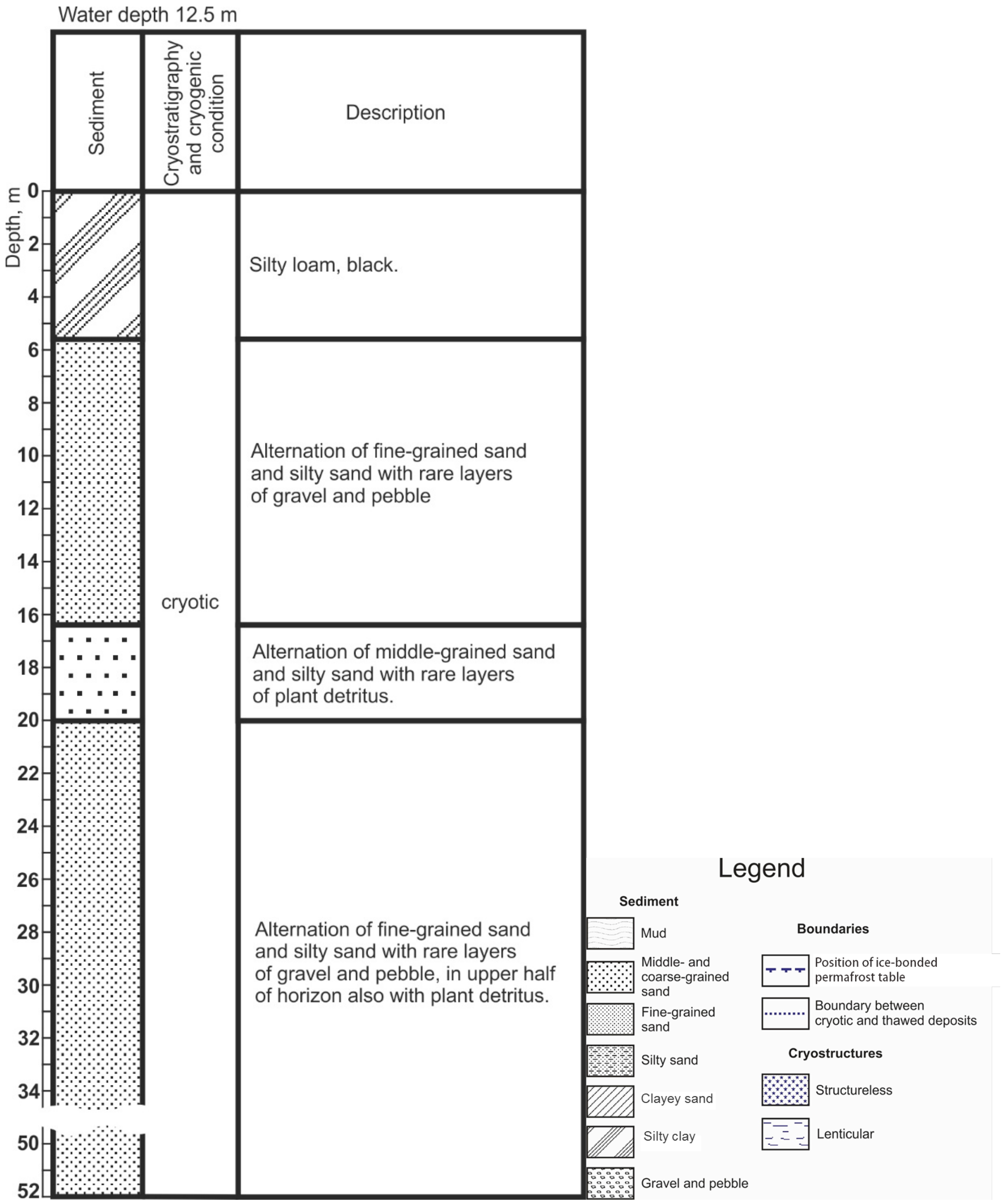

Figure S1: Lithology and cryostratigraphy of the sediment core recovered from the borehole ID-11 in the near-shore zone of the ESAS. Ice-bonded permafrost table was not reached during the drilling. The sediments from 0 to 52 m below the seafloor were cryotic, that is unfrozen under temperatures <0°C.

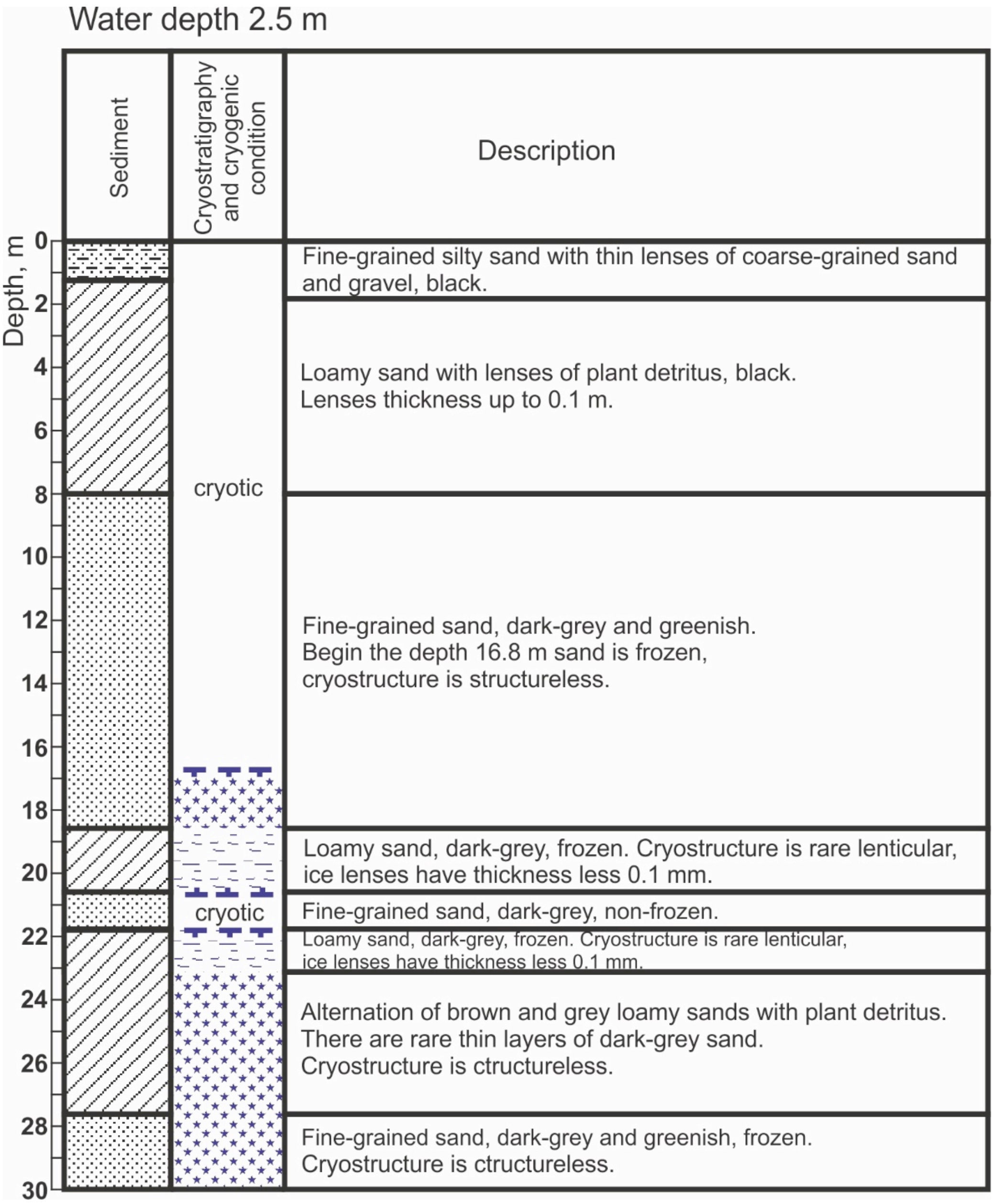

Figure S2. Lithology and cryostratigraphy of the sediment core recovered from the borehole IID-13 in the near-shore zone of the ESAS. Ice-bonded permafrost table was reached at 16.4 m below the seafloor during the drilling. The sediments from 0 m to 16.4 m below the seafloor were cryotic, that is unfrozen under temperatures <0°C. A thin layer (1.2 m) of cryotic sediments was also observed at depth of 20.5 m below the seafloor. Legends, see Fig. S1.

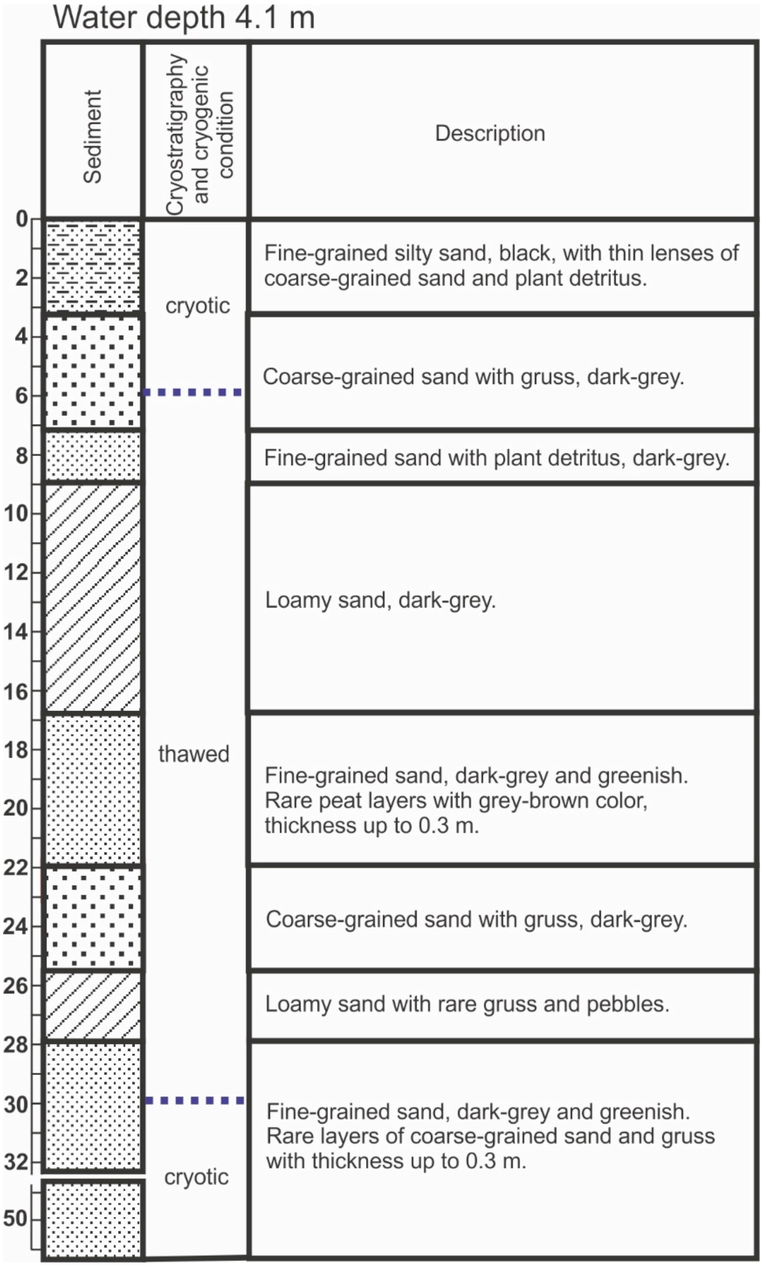

Figure S3. Lithology and cryostratigraphy of the sediment core recovered from the borehole IIID-13 in the near-shore zone of the ESAS. Ice-bonded permafrost table was not reached during the drilling. The sediments from 0 m to 51 m below the seafloor were cryotic from 0 to 6 m below the seafloor; thawed (that is unfrozen under temperatures >0°C) from 6 to 30 m below the seafloor and cryotic from 30 to 51 m below the seafloor. Legends, see Fig. S1.

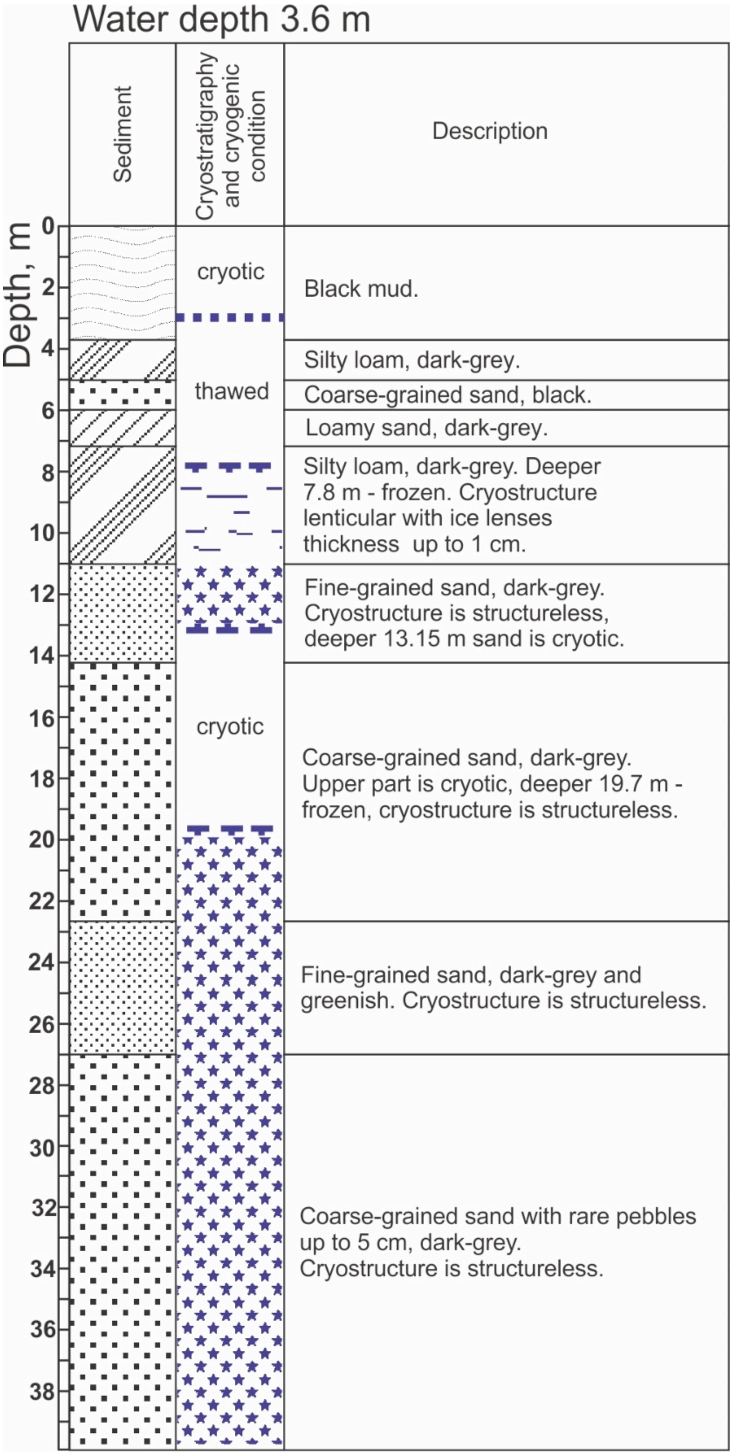

Figure S4. Lithology and cryostratigraphy of the sediment core recovered from the borehole VD-13 in the near-shore zone of the ESAS. Ice-bonded permafrost table was reached at 7.8m below the seafloor during the drilling. The sediments from 0 m to 3 m below the seafloor were cryotic; from 3 to 7.8 – frozen; within frozen sediments, the layer of cryotic sediments was observed from 13 to 19.5 m below the seafloor. Legends, see Fig. S1.

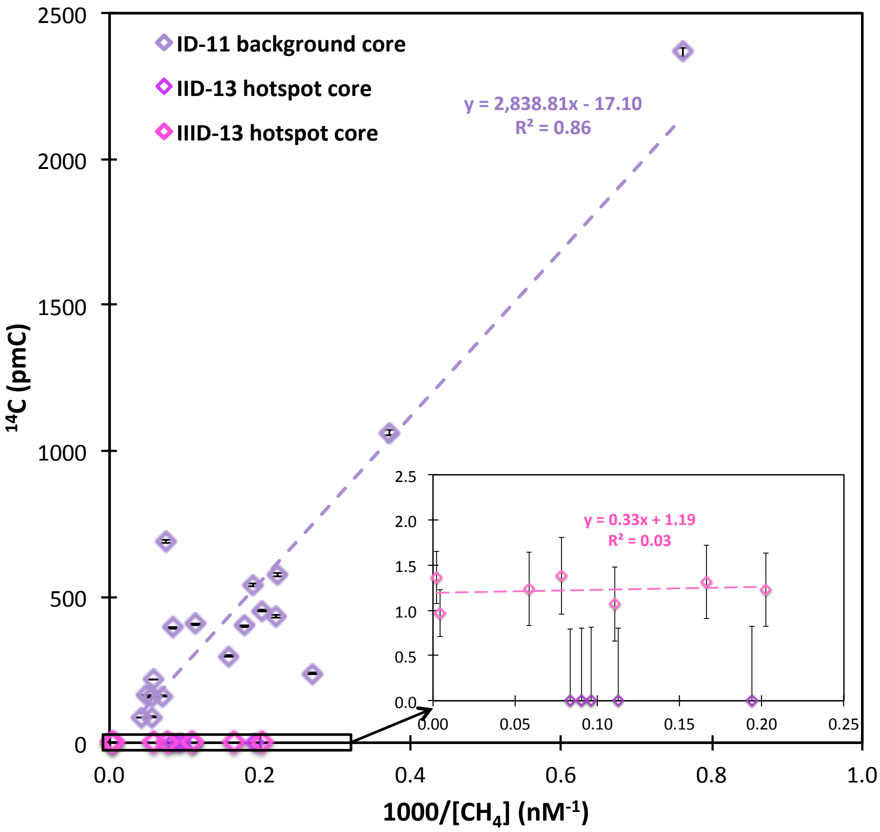

Figure S5: Keeling plot: inverse CH_4 concentration versus ^{14}C data for sediment samples in the partially thawed subsea permafrost. The diamonds are "deep" core sediment data and the dashed lines represent the linear regressions for the ID-11 (purple) and IIID-13 (pink) cores. All values of the IID-13 core are close to zero so no linear regression line is depicted for this core. The intersections with the y-axis correspond to the ^{14}C pmC values of the main CH_4 substrate.